

A substrate-versatile catalyst for the selective oxidation of light alkanes I. Reactivity

Joseph H. Holles,^a Christopher J. Dillon,^a Jay A. Labinger,^b and Mark E. Davis^{a,*}

^a *Chemical Engineering, California Institute of Technology, Pasadena, CA 91125, USA*

^b *Beckman Institute, California Institute of Technology, Pasadena, CA 91125, USA*

Received 17 September 2002; revised 11 December 2002; accepted 16 December 2002

Abstract

The reactivity of niobium and pyridine-exchanged molybdophosphoric (NbPMo₁₂pyr) and molybdovanadophosphoric (NbPMo₁₁Vpyr) acid catalysts are investigated for the selective oxidation of light alkanes. Productivities and selectivities are presented for the reactions of propane to acrylic acid and *n*-butane to maleic acid. Pretreatment of the material to 420 °C in an inert atmosphere is required to form an active catalyst, and the combination of both niobium and pyridine is necessary for obtaining maximum activity. Vanadium is not essential for the selective formation of maleic acid from butane, but does appear to affect the selective formation of acrylic acid from propane. Other metal cations can be used instead of niobium; however, none are as effective as niobium. Comparison of activity results to those from other molybdate-based structures indicates that high activity requires the use of a reducible molybdenum species. In addition, the central phosphorus heteroatom of the polyoxometalate is important for high activity. Structures without phosphorus or with other heteroatoms have lower activity. The catalysts are effective under both hydrocarbon-rich and oxygen-rich conditions. For butane, the productivity to maleic acid exceeds that of the current industrial standard vanadium phosphorus oxide. With propane, the productivity to acrylic acid is above that of the MoVNbTe mixed-metal oxide. In addition to efficiently catalyzing the selective oxidation of propane and butane, the catalysts are active with feeds containing other substrates such as ethane, isobutane, and toluene.

© 2003 Elsevier Inc. All rights reserved.

Keywords: Heterogeneous catalysis; Selective oxidation; Propane; *n*-Butane; Polyoxometalate; Keggin unit; Wells–Dawson unit; Strandberg unit; Niobium; Pyridine

1. Introduction

Catalytic selective oxidation processes are a mainstay of the modern chemical industry. Today, more than 60% of the chemicals and intermediates synthesized via catalytic processes are products of oxidation [1]. One area of selective oxidation that has received a continuing focus is the selective oxidation of light alkanes [2]. This is due to the abundance and low cost of the light alkanes such as ethane, propane, and butane.

The conversion of *n*-butane to maleic anhydride over vanadium phosphorus oxide (VPO) catalysts with molecular oxygen is a well-established commercial process [1]. This process typically achieves conversions of around 75% and selectivities near 67%. Selective oxidation of *n*-butane is

still the only example of an industrial, selective catalytic oxidation process that uses an alkane as a feedstock [3].

Other selective oxidation reactions of interest include the production of acetic acid from ethane and acrylic acid from propane. In contrast to *n*-butane, the VPO catalysts are not effective for these substrates [4]. For ethane, the most common catalyst system is a MoVNb mixed-metal oxide that produces mostly ethylene [5]; however, titania-supported VP oxides have recently been reported to produce significant amounts of acetic acid [6]. The most active catalysts for conversion of propane to acrylic acid are even more complex mixed-metal oxides such as MoVNbTe [7,8] and MoVNbSb [9].

Heteropolyacids and their polyoxometalate derivatives have received extensive study for many different catalytic applications. These materials are often effective due to their bifunctional nature as both acid and oxidation catalysts. Indeed, polyoxometalates, and phosphomolybdates, in particular, have been extensively investigated for the selective

* Corresponding author.

E-mail address: mdavis@cheme.caltech.edu (M.E. Davis).

oxidation of light alkanes [10–12]. Most of these studies have focused on the effect of different exchange cations or the incorporation of different amounts of vanadium in the polyoxometalate structure. An advance in this field is the work of Ueda and Suzuki, who demonstrated that a molybdovanadophosphoric acid (denoted as PMo_{11}V) treated with pyridine resulted in a active and selective catalyst for the conversion of propane to acrylic acid [13]. Subsequently, Li and Ueda found that treating molybdophosphoric acid (denoted as PMo_{12}) with pyridine and then activating in nitrogen at 420 °C improved activity for the selective oxidation of propane to acrylic acid [14].

Recently, we reported on niobium and pyridine-exchanged molybdophosphoric and molybdovanadophosphoric acid catalysts ($\text{NbPMo}_{12}\text{pyr}$ and $\text{NbPMo}_{11}\text{Vpyr}$) for selective oxidation of propane and butane [15]. Here, we describe further this first example of a substrate versatile catalyst for selective oxidation. Part I reports the reactivity studies in order to define the components that are necessary for good activity and selectivity. Part II then provides characterizations of the better catalytic materials illustrated in Part I.

2. Experimental

2.1. Catalyst preparation

2.1.1. $\text{NbPMo}_{12}\text{pyr}$

Molybdophosphoric acid (PMo_{12}) was purchased from Aldrich. Niobium pentachloride (1.210 g) was dissolved in water (10 mL) and the solution basified with ammonium hydroxide (0.5 mL). The white precipitate was removed by filtration and dissolved in aqueous oxalic acid (1.008 g in 20 mL water). The niobium oxalate solution was then slowly added to PMo_{12} (20 g) dissolved in water (40 mL). The mixture was stirred and heated to 80 °C until the liquid had evaporated. An aqueous solution of pyridine (1.645 g in 10 mL water) was slowly added to a slurry of the resulting niobium polyoxometalate (NbPMo_{12}) (5.260 g) in water (30 mL) to form an immediate precipitate. The mixture was stirred and evaporated to dryness at 80 °C.

Other metal-exchanged phosphomolybdates ($\text{MPMo}_{12}\text{pyr}$) were prepared similarly. For $\text{MoPMo}_{12}\text{pyr}$, ammonium molybdate ($(\text{NH}_4)_2\text{MoO}_4$) (0.082 g) was dissolved in water and stirred with Dowex 50 \times 8-200 proton form ion-exchange resin (0.17 g) for 1.5 h. The resin was filtered off and oxalic acid (0.073 g) was added. The molybdenum oxalate solution was then added to molybdophosphoric acid (1.5 g) and exchanged with pyridine as above. For $\text{ZrPMo}_{12}\text{pyr}$, zirconium sulfate $\text{Zr}(\text{SO}_4)_2$ (0.292 g) was dissolved in water (20 mL) and basified with ammonium hydroxide. The white precipitate was removed by filtration and dissolved in oxalic acid (0.187 g in 20 mL water). The zirconium oxalate solution was then slowly added to PMo_{12} (1.5 g) dissolved in water (40 mL) and evaporated and pyridine-exchanged as above. For $\text{TiPMo}_{12}\text{pyr}$, titanium

oxalate (0.064 g) was dissolved in water (20 mL); the solution was then added to PMo_{12} (0.75 g) dissolved in water (40 mL) and pyridine-exchanged. For $\text{VPMo}_{12}\text{pyr}$, vanadium pentoxide V_2O_5 (0.046 g) was dissolved in water (40 mL) and then added to oxalic acid in water (0.136 g in 10 mL). This solution was then added to PMo_{12} (1.5 g) dissolved in water (40 mL) and pyridine-exchanged. For $\text{CrPMo}_{12}\text{pyr}$, chromium trioxide CrO_3 (0.051 g) was dissolved in water (10 mL) and then added to oxalic acid in water (0.182 g in 10 mL). This solution was then added to PMo_{12} (1.5 g) dissolved in water (40 mL) and pyridine-exchanged.

2.1.2. $\text{NbPMo}_{11}\text{Vpyr}$

Molybdovanadophosphoric acid (PMo_{11}V) was prepared by a known literature method [16]. Sodium hydrogen phosphate Na_2HPO_4 (7.098 g) was dissolved in 100 mL distilled water at room temperature. Sodium metavanadate NaVO_3 (6.097 g) was dissolved in 100 mL of water at 80 °C. The two solutions were combined at room temperature and acidified with concentrated sulfuric acid (5 mL) which led to a dark red solution. Sodium molybdate dihydrate $\text{Na}_2\text{MoO}_4 \cdot 2\text{H}_2\text{O}$ (133.1 g) was dissolved in 200 mL water and then the two solutions were combined, whereupon the Keggin unit self-assembled in solution.

The sodium form of the Keggin anion was proton-exchanged by adding concentrated sulfuric acid (85 mL) to the solution for 90 min (exotherm) with vigorous stirring. This generated a clear bright red solution that was added to diethyl ether (200 mL) in a separating funnel and shaken. Three phases resulted, from which the dark red layer was decanted and retained. The aqueous layer was extracted twice with ether, and the ethereal fractions were combined. The diethyl ether was removed under vacuum resulting in a thick red syrup that was dissolved in water and recrystallized. The orange crystals of PMo_{11}V were dried overnight at 100 °C, and then niobium- and pyridine-exchanged as above.

2.1.3. $\text{NbP}_2\text{Mo}_{18}\text{pyr}$

Sodium hydrogen phosphate $\text{Na}_2\text{HPO}_4 \cdot 12\text{H}_2\text{O}$ (7.14 g) was dissolved in a mixture of perchloric acid (75 mL) and water (50 mL). The solution was cooled to 20 °C. Then a solution of sodium molybdate $\text{Na}_2\text{MoO}_4 \cdot 2\text{H}_2\text{O}$ (108.27 g) in water (200 mL) was added dropwise to the above solution. The resulting solution was clear yellow. The solution was allowed to evaporate in air and after 2 weeks yellow crystals of $\text{Na}_6\text{P}_2\text{Mo}_{18}\text{O}_{62}$ formed [17]. Formation of the Wells–Dawson unit was confirmed by single-crystal diffraction. The crystals were filtered off and proton-, niobium-, and pyridine-exchanged as above.

2.1.4. $\text{NbP}_2\text{Mo}_5\text{pyr}$

Sodium molybdate $\text{Na}_2\text{MoO}_4 \cdot 2\text{H}_2\text{O}$ (24.682 g) and sodium dihydrogen phosphate $\text{NaH}_2\text{PO}_4 \cdot 2\text{H}_2\text{O}$ (6.369 g) were added to 10.5 mL of perchloric acid. Distilled water

was added to increase the total volume to 50 mL and the solution was stirred to aid dissolution. The resulting solution was clear. The solution was allowed to evaporate in air and after 2 weeks clear crystals of $\text{Na}_6\text{P}_2\text{Mo}_5\text{O}_{23}$ formed [18]. Formation of the Strandberg unit was confirmed by single-crystal diffraction. The sodium form was then converted to an exchangeable form by dissolving 4.008 g in 20 mL water and adding Dowex 50 \times 8-200 ion-exchange resin (1.567 g) and stirring for 90 min to form $\text{Na}_4\text{H}_2\text{P}_2\text{Mo}_5\text{O}_{23}$. The resin was filtered off and the sample subsequently niobium- and pyridine-exchanged as above. Stability of the Strandberg unit throughout the synthesis procedure was confirmed by the presence of a ^{31}P NMR peak at approximately 2 ppm [19].

2.1.5. NbMo_8pyr

The procedure of Gili et al. was adapted for pyridine [20]. An aqueous solution of pyridine (1.931 g in 120 mL of distilled water) was added to an aqueous suspension of MoO_3 (3.213 g of MoO_3 in 1800 mL of distilled water). The mixture was heated under reflux with stirring for 6 h, cooled in an ice bath, and filtered. The solution was then reduced to 600 mL by a rotary evaporator and allowed to stand overnight whereupon a white precipitate ($\text{C}_5\text{H}_5\text{NH}$) $_4$ (Mo_8O_{26}) formed. The crystals were filtered, washed with water, and dried. Powder diffraction and TGA curves were identical to those of McCarron et al. [21]. The sample was niobium-exchanged as above.

2.1.6. $\text{PMo}_{11}\text{Nbpyr}$

Molybdophosphoric acid (2.7 mmol; 5.00 g) was dissolved in water (27.4 mL). The pH of the solution was then adjusted to 4.4 using Li_2CO_3 (0.583 g) to form a lacunary Keggin ion structure [22]. One molar equivalent of niobium oxalate was added to the solution. The solution was stirred for 2 h to form molybdoniobophosphoric acid $\text{PMo}_{11}\text{NbO}_{40}$. Pyridine was added (0.216 g) and a yellow precipitate was formed, filtered off, and dried.

2.1.7. $(\text{VO})\text{PMo}_{11}\text{Nbpyr}$

From molybdophosphoric acid (5.00 g), molybdoniobophosphoric acid was made in solution as described above, to which an aqueous solution of vanadyl oxalate (0.213 g) was added to form a dark green solution. The addition of pyridine (0.216 g) to the solution caused the precipitation of a pale green solid that was removed by filtration and allowed to air dry.

2.2. Reactivity studies

Experiments were performed in a BTRS Jr. reactor (Autoclave Engineers) with a stainless-steel reactor tube. A 0.2 g (\sim 0.2 mL) catalyst (35–60 mesh) was mixed with 1 mL silicon carbide (16 mesh, Abrasives Unlimited) and held in the reactor with glass wool. Reactant flow was single pass. The catalyst sample was pretreated by

heating to 420 °C for 5 h and then held for 6 h at that temperature before cooling to 380 °C in flowing He. This treatment removes all organic components from the catalyst precursors [15]. Feed gases included *n*-butane (99.9%, Matheson), oxygen (99.5%, Air Liquide), and 5% argon in helium (99.999%, Air Liquide). Standard flow rates were 4:2:4:5 mL min $^{-1}$ of *n*-butane:oxygen:argon/helium:steam. Water was injected to the reactor feed flow via a syringe pump to form steam. Total pressure in the reactor was atmospheric and no pressure drop across the reactor was observed. Standard reaction temperature was 380 °C.

Feed to the reactor was initiated and allowed to come to steady-state for 1 h. At this point sampling was initiated. Reported data are the average values for the second hour on stream. Reaction experiments were typically performed for 10 h, however, a single run with propane was accomplished for 72 h without loss of activity. Reactant and product analysis was by GCMS using a HP GCD Plus with a HP-Plot Q column. Gas analysis was performed online while oxygenated products were trapped in an ice bath and analyzed offline. Experiments using ethane (99.99%, Matheson), propane (99.98%, Matheson), and isobutane (99%, Matheson) were performed similarly. For the toluene experiment, the helium/oxygen reactant was fed through a bubbler containing toluene (99.8%, Aldrich) at room temperature. Product selectivities are reported in mole percentages.

Surface area measurements (BET) were performed on a Coulter Omnisorp 100 using nitrogen (99.996%, Air Liquide) adsorption at 77 K. Surface areas were determined after pretreating to 420 °C.

Elemental analysis was performed by Galbraith Laboratories Inc. (Knoxville, TN).

3. Results

3.1. *n*-Butane reactivity

Previously, the importance of vanadium, niobium, and pyridine on the *n*-butane reactivity was determined by investigating a series of catalysts that were systematically prepared to incorporate all combinations of the three components [15]. Results from those and further studies of this catalyst system are reported in Table 1 (products trapped in water that presumably convert maleic anhydride to maleic acid). All results are for 0.2 g catalyst at 380 °C under hydrocarbon-rich conditions ($\text{C}_4/\text{O}_2 = 2/1$). The samples that contain both niobium and pyridine are the most active and selective (15% butane conversion is the maximum possible under these conditions). These materials are also capable of maintaining high conversion and selectivity even when increasing the total flow rate by a factor of 8 (compare lines 5 and 6). In contrast, the samples that do not contain pyridine exhibit very low activity. The solids that contain pyridine but no niobium have intermediate activity, and are not capable of maintaining high conversion under increased flow rates

Table 1
Catalyst reactivity using *n*-butane as substrate

Catalyst	Flow (mL min ⁻¹) ^a	Conversion (%)		Selectivity (%) ^b				STY ^c
		C ₄	O ₂	CO _x	Ac	AA	MA	
PMo ₁₂	4:2:4:5	0.2	7	64	34	2	0	0
NbPMo ₁₂	4:2:4:5	3	32	13	7	2	70	0.017
PMo ₁₂ pyr	4:2:4:5	13.5	89	14	3	1	82	0.097
	32:16:32:40	2.5	17	9	6	6	71	0.11
NbPMo ₁₂ pyr	4:2:4:5	15	100	25	3	1	71	0.084
	32:16:32:40	15	100	5	3	1	90	0.84
	64:32:64:80	9	60	17	12	13	49	0.56
PMo ₁₁ V	4:2:4:5	0.5	9	31	17	0	50	1.6 × 10 ⁻³
NbPMo ₁₁ V	4:2:4:5	0.4	9	42	19	4	25	6.3 × 10 ⁻⁴
PMo ₁₁ Vpyr	4:2:4:5	13.5	90	5	3	1	90	0.11
	32:16:32:40	14	95	9	5	3	80	0.76
NbPMo ₁₁ Vpyr	4:2:4:5	15	100	16	5	2	76	0.090
	32:16:32:40	14	95	9	5	3	80	0.76
	64:32:64:80	12.3	82	33	5	3	57	0.89

Some of the data in this table have been previously reported [15]. All at 380 °C with 0.2 g catalyst.

^a *n*-Butane:oxygen:helium:water.

^b C₄, *n*-butane; CO_x, carbon oxides; Ac, acetic acid; AA, acrylic acid; MA, maleic acid.

^c Space-time yield of maleic acid (mmol min⁻¹ (g of catalyst)⁻¹).

(compare lines 3 and 4). Surface area measurements for the series of materials listed in Table 1 are reported in Table 2. The surface area of the most active catalyst, NbPMo₁₁Vpyr, is roughly a factor of 2 greater than the acid form of the material (PMo₁₁V).

The active catalysts containing both niobium and pyridine perform well under different reaction conditions, as shown by the data in Table 3. The first three entries demonstrate the effect of changing the oxygen partial pressure in a hydrocarbon-rich reactant mixture. These studies were performed at low temperatures and low levels of conversion in order to prevent complete conversion of oxygen. Comparing entries 1 and 2 shows that doubling the oxygen partial pressure by changing the flow rate from 8 to 16 mL min⁻¹ results in doubling the conversion of butane and space-time yield of maleic acid, while reducing the oxygen flow to 2 mL min⁻¹ caused no significant change in butane conversion and some decrease in space-time yield. Entries 4 and 5 in Table 3 list the activity of NbPMo₁₁Vpyr under conditions comparable to those used in industry (VPO catalysts are used in considerably more oxygen-rich reaction mixtures at high butane conversion levels). Under these conditions, CO_x and maleic acid each accounted for around half of the product effluent at 340 and 300 °C. The remaining entries in Table 3 provide additional reactivity data for NbPMo₁₁Vpyr and NbPMo₁₂pyr

Table 2
Surface area measurements

Sample	Surface area (m ² /g)
PMo ₁₂	7.7
PMo ₁₁ V	5.9
NbPMo ₁₁ V	7.0
PMo ₁₁ Vpyr	17
NbPMo ₁₁ Vpyr (as prepared)	4.8
NbPMo ₁₁ Vpyr	10

All samples, except as noted, activated at 420 °C.

showing that over the temperature range 300 to 420 °C the selectivity to maleic acid remains at 60% or higher.

Table 4 compares the reactivity of *n*-butane over the niobium/pyridine polyoxometalate catalysts to several of the catalyst systems reported in the literature, including both commercial VPO and the best heteropolyacid-based catalysts. The niobium/pyridine catalysts exhibit substantially higher space-time yields than VPO with similar selectivities. Even under the more typical oxygen-rich industrial conditions, the new catalyst performs well. When compared to the heteropolyacid-based catalysts from the literature, the niobium/pyridine system is dramatically more active.

In order to determine whether the Keggin structure (Fig. 1a) of the niobium/pyridine phosphomolybdate is essential for the activity, a series of structural variations, all based on MoO₆ octahedral units, were examined. Results from bulk MoO₃, the octamolybdate species (Mo₈O₂₆) (Fig. 1b), the Wells–Dawson (P₂Mo₁₈) unit (Fig. 1c), and the Strandberg (P₂Mo₅) unit (Fig. 1d) are given in Table 5. MoO₃ alone shows little activity and no selectivity to maleic acid, while a physical mixture of molybdenum, vanadium, and niobium oxides produces a selectivity to maleic acid of 20%. The octamolybdate with niobium and pyridine produces around half the activity obtained for NbPMo₁₂pyr. The activity of the Wells–Dawson unit is essentially the same as the Keggin unit while the Strandberg unit gives no selectivity to maleic acid at all.

Instead of ion exchanging niobium into the sample, we have been able to incorporate it in the Keggin unit as a framework atom. This incorporation of niobium into a phosphomolybdate heteropolyacid (PMo₁₁Nbpyr) is new and is discussed in Part II [23]. The productivity from this sample (lines 10 and 11) was similar to the niobium-exchanged Keggin analogue or Wells–Dawson unit. A central silicon atom in place of the phosphorus atom in the Keggin unit results

Table 3
n-Butane reactivity under different reaction conditions

Catalyst	Flow (mL min ⁻¹) ^a	<i>T</i> (°C)	Conversion (%)		Selectivity (%)				STY ^b
			C ₄	O ₂	CO _x	Ac	AA	MA	
NbPMo ₁₁ Vpyr ^c	16:8:16:20	300	1.8	27	34	6	2	50	6.4 × 10 ⁻²
NbPMo ₁₁ Vpyr ^c	16:16:16:20	300	3.7	25	26	6	2	61	0.14
NbPMo ₁₁ Vpyr ^c	16:2:16:20	300	2.1	62	33	7	1	50	3.7 × 10 ⁻²
NbPMo ₁₁ Vpyr ^d	1:10:35:5	300	29	33	51	5	1	44	6.4 × 10 ⁻³
NbPMo ₁₁ Vpyr ^d	1:10:35:5	340	62	61	50	4	1	46	1.9 × 10 ⁻²
NbPMo ₁₁ Vpyr ^d	2:10:35:5	340	63	81	54	4	1	41	3.0 × 10 ⁻²
NbPMo ₁₂ pyr ^c	32:16:32:40	340	13.5	90	5	4	1	89	0.76
NbPMo ₁₁ Vpyr ^c	8:4:8:10	340	14	95	24	11	3	62	0.14
NbPMo ₁₁ Vpyr ^c	4:2:4:5	300	9	75	26	12	2	60	0.05
NbPMo ₁₁ Vpyr ^c	256:128:256:80	420	6.9	46	22	3	3	68	2.37

^a *n*-Butane:oxygen:helium:water.

^b Space-time yield of maleic acid (mmol min⁻¹ (g of catalyst)⁻¹).

^c 0.2 g catalyst.

^d 0.99 g catalyst.

in a high selectivity to CO_x and a low space-time yield of maleic acid.

In addition to niobium, other metals can be ion-exchanged to the PMo₁₂pyr, including Ti, V, Cr, Fe, Cu, Y, Zr, Sb, Ce, and Bi. Results for the most active of these samples are reported in Table 6. The niobium catalyst is still the most active, by a factor of 2 compared to titanium and molybdenum. Chromium and zirconium also demonstrated some activity. Although vanadium and niobium are in the same column in the periodic table, the vanadium catalyst did not perform nearly as well.

Further attempts to optimize the catalyst activity by varying the amount of niobium and pyridine present are shown in Fig. 2. Catalyst samples were prepared with 0.04 to 0.98 niobium atoms per phosphorus atom (or Keggin unit) with the pyridine balancing the remainder of the charge. The most active sample contained 0.30 niobium atoms per Keggin unit, with all samples having similar selectivities.

Instead of using pyridine to activate the sample, other reducing atmospheres were investigated. Carbon monoxide, ammonia, and hydrogen gas were used to pretreat NbPMo₁₁V. Results from these experiments are shown in

Table 7. Ammonia and hydrogen pretreatments had little effect while CO was able to increase the activity by two orders of magnitude compared to a pyridine-free sample. However, this is still one order of magnitude lower than the pyridine-containing sample. Attempts to combine the pyridine and CO activation were unsuccessful, resulting in a decrease in activity.

3.2. Propane reactivity

Propane reactivity was determined over a series of catalysts where each of the three different additives was systematically incorporated. In addition, a material was prepared that incorporated niobium into the structure and was ion-exchanged with the vanadium species. Results for these samples are shown in Table 8. As with butane, the catalysts that contain both niobium and pyridine are the most active [15]. However, in contrast with butane, the presence of vanadium does strongly affect the reactivity results primarily by increasing the selectivity to acrylic acid. The method of introducing vanadium may be important as well: (VO)PMo₁₁Nbpyr gives somewhat lower selectivity to

Table 4
 Comparison of *n*-butane reactivity to literature data

Catalyst	Flow (mL min ⁻¹) ^a	<i>T</i> (°C)	Conversion (%)		Selectivity (%)		STY ^c	Rate (mmol min ⁻¹ m ⁻²)	Ref.
			C ₄	O ₂	CO _x	MA ^b			
NbPMo ₁₂ pyr	32:16:32:40	380	15	100	5	90	0.84	8.4 × 10 ⁻²	This work
NbPMo ₁₁ Vpyr	1:10:35:5	340	62	61	50	46	0.019	1.9 × 10 ⁻³	This work
VPO	4:6:26:0	380	30	–	10	80	0.067	3.0 × 10 ⁻³	[27]
VPOCo	4:2:2.4:18.4:0	400	25.5	77.9	46.2	11.5	0.022	7.9 × 10 ⁻⁴	[30]
BiPMo ₁₂ + 2VO ²⁺	6.3:58:218:34	360	31.8	–	37	32	1.3 × 10 ⁻³	–	[11]
PMo ₁₀ V ₂	0.6:5.4:24:0	340	90	–	–	38	2.8 × 10 ⁻³	–	[10]

Some of the data in this table have been previously reported [15].

^a *n*-Butane:oxygen:helium:water.

^b MA, maleic acid or maleic anhydride.

^c Space-time yield of maleic acid (mmol min⁻¹ (g of catalyst)⁻¹).

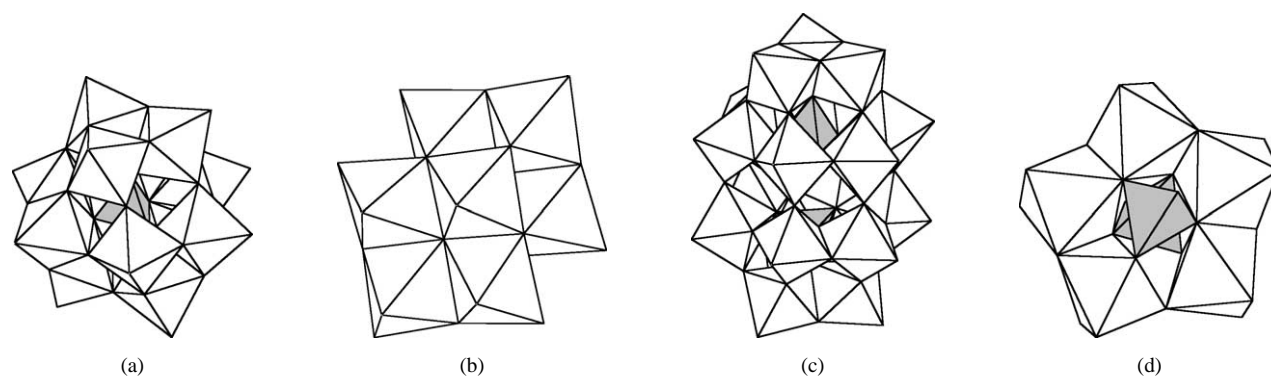


Fig. 1. Anion structures: (a) $\text{PMo}_{12}\text{O}_{40}^{3-}$ Keggin unit, (b) $\text{Mo}_8\text{O}_{26}^{4-}$ octamolybdate, (c) $\text{P}_2\text{Mo}_{18}\text{O}_{62}^{6-}$ Wells–Dawson unit, and (d) $\text{P}_2\text{Mo}_5\text{O}_{23}^{6-}$ Strandberg unit. Molybdenum atoms are located near the center of the white octahedra with oxygen atoms at the corners. A phosphorus atom is located at the center of the shaded tetrahedron with oxygen atoms at the corners.

acrylic acid than $\text{NbPMo}_{11}\text{Vpyr}$. Note that these catalysts produce substantial amounts of maleic acid in addition to the expected products of acetic and acrylic acid.

Selectivity also depends on flow rate. As shown in entries 1 and 2 of Table 9, increasing the total flow rate fourfold causes the selectivity of acrylic acid to increase from 21 to 49%, while selectivity to maleic acid decreases from 43 to 15%. Good selectivities and yields are also obtained at lower temperatures (Table 9).

Table 10 compares the reactivity of propane over the niobium/pyridine polyoxometalate materials to several catalysts reported in the literature. These include the MoVNb -based mixed-metal oxides as well as a heteropolyacid-based catalyst. For comparison, reactivity results with the $\text{NbPMo}_{11}\text{Vpyr}$ sample under oxygen-rich conditions are also included. Since the literature data are at different temperatures, flow rates, and residence times, direct comparisons are difficult. However, while the $\text{NbPMo}_{11}\text{Vpyr}$ catalyst is not the

most selective, it has a very high space-time yield compared to the other catalysts.

3.3. Other reactants

Reactivity data for ethane, isobutane, and toluene are shown in Table 11. Comparisons to other catalyst systems reported in the literature for each of the three substrates are also included. For ethane, the space-time yield to ethylene and acetic acid from the $\text{NbPMo}_{11}\text{Vpyr}$ compare well to vanadium oxide supported on titania and the MoVNb mixed-metal oxide catalysts. Other MoVNb -based systems specifically designed to produce ethylene or acetic acid are also shown. Similarly, the $\text{NbPMo}_{11}\text{Vpyr}$ catalyst has a good space-time yield of methacrylic acid from isobutane. However, the selectivity is very low for this sample (mostly deep oxidation products). Finally, space-time yields to benzoic acid and benzaldehyde from toluene are less than those reported for a AgVCe mixed-metal oxide.

Table 5
Reactivity of solids containing Mo-oxide structural variations

Catalyst	Flow (mL min^{-1}) ^a	Conversion (%)		Selectivity (%)		STY ^b
		C ₄	O ₂	CO _x	MA	
MoO_3	4:2:4:5	0.7	20	95	0	0
Phys. Mix. ^c	4:2:4:5	12	95	60	20	0.023
$\text{PMo}_{12}\text{pyr}$	4:2:4:5	13.5	89	14	82	0.097
$\text{NbMo}_8\text{O}_{26}\text{pyr}$	4:2:4:5	15	100	50	37	0.044
	27:16:32:40	5	49	28	56	0.219
$\text{NbPMo}_{12}\text{pyr}$	4:2:4:5	15	100	22	71	0.084
	64:32:64:80	7.4	52	19	52	0.52
$\text{NbP}_2\text{Mo}_{18}\text{pyr}$	4:2:4:5	15	100	26	65	0.077
	64:32:64:80	7.4	52	16	52	0.52
$\text{PMo}_{11}\text{Nbpyr}$	4:2:4:5	15	100	12	62	0.073
	64:32:64:80	12.5	83	36	39	0.61
$\text{NbP}_2\text{Mo}_5\text{pyr}$	4:2:4:5	2	25	81	0	0
$\text{NbSiMo}_{12}\text{pyr}$	4:2:4:5	11	80	69	18	0.017

All at 380 °C with 0.2 g catalyst.

^a *n*-Butane:oxygen:helium:water.

^b Space-time yield of maleic acid ($\text{mmol min}^{-1} (\text{g of catalyst})^{-1}$).

^c Physical mixture of MoO_3 , V_2O_5 , Nb_2O_5 , and pyridine with the same stoichiometric ratios as $\text{NbPMo}_{11}\text{Vpyr}$.

Table 6
Reactivity of $\text{MPMo}_{12}\text{pyr}$ with different exchange cations

M	Flow (mL min^{-1}) ^a	Conversion (%)		Selectivity (%)		STY ^b
		C ₄	O ₂	CO _x	MA	
Nb	32:16:32:40	15	100	22	71	0.67
Ti	32:16:32:40	8	60	24	69	0.39
Mo	32:16:32:40	7	51	11	79	0.38
Cr	27:16:32:40	6	43	15	81	0.23
Zr	16:8:16:20	7	41	9	83	0.17
V	8:4:8:10	7	61	22	54	0.08

All at 380 °C with 0.2 g catalyst.

^a *n*-Butane:oxygen:helium:water.

^b Space-time yield of maleic acid (mmol min^{-1} (g of catalyst)⁻¹).

4. Discussion

The addition of niobium and pyridine to the phosphomolybdate Keggin ion leads to a catalyst achieving greatly enhanced productivity of maleic acid from *n*-butane. While PMo_{11}V demonstrates some activity for maleic acid, PMo_{12} produces no maleic acid. Niobium and pyridine individually promote the reaction (the individual effect of pyridine is greater than that of niobium), and the addition of both niobium and pyridine increases the activity of PMo_{11}V by almost three orders of magnitude. In addition to increasing productivity, pyridine and niobium do not appear to have an adverse effect on selectivity. In contrast, the addition of vanadium appears to have only a minimal effect on productivity for the most active catalyst, but does affect selectivity: $\text{NbPMo}_{11}\text{Vpyr}$ produces more CO_x while $\text{NbPMo}_{12}\text{pyr}$ produces more acetic and acrylic acid under high flow rate conditions. It is important to note that this dramatic increase in activity is not simply the result of increased surface area. Although the surface area does increase with the incorporation of pyridine, it is only by about a factor of 2. This suggests that the addition of niobium and pyridine to the heteropolyacid has a chemical effect on the active state.

The multisubstrate usefulness of this catalyst is clearly demonstrated by the results for the selective oxidation of propane to acrylic acid. While PMo_{11}V shows no activity, both $\text{NbPMo}_{11}\text{V}$ and $\text{PMo}_{11}\text{Vpyr}$ reveal some activity for the production of acrylic acid. Again, the individual effect of pyridine is larger than that of niobium, and as with butane, the combination of both niobium and pyridine produces the

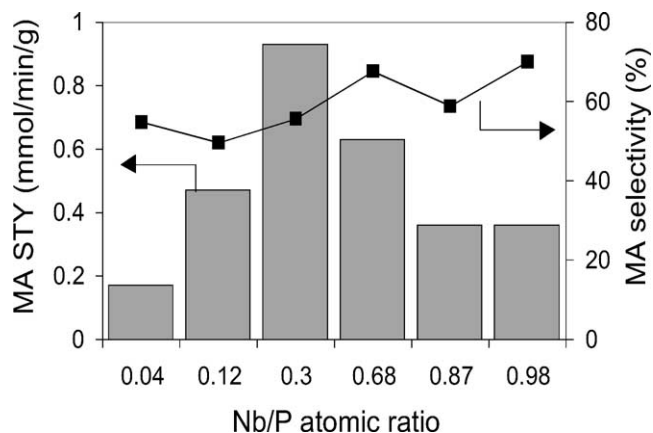


Fig. 2. Selectivity and space-time yield of $\text{NbPMo}_{11}\text{Vpyr}$ catalysts to maleic acid as a function of niobium loading.

most active catalyst. In contrast to the butane results, vanadium has a significant effect on the reactivity of propane. Without vanadium, catalysts containing niobium and pyridine exhibit a high selectivity to complete oxidation products, regardless of whether niobium is synthesized in the Keggin unit or ion-exchanged. In addition, $\text{NbPMo}_{11}\text{Vpyr}$ and $(\text{VO})\text{PMo}_{11}\text{Nbpyr}$ differ only by about a factor of 2 in acrylic acid productivities, suggesting that the position where each component is initially located in the precursor material has some effect (but not a critical one) and that each species is able to move to its final position during pre-treatment. X-ray absorption spectroscopy evidence supporting this conclusion is provided in the following paper [23]. A similar result has been reported for a *n*-butane catalyst system, where exchanged and Keggin substituted vanadium samples showed very similar activities [11].

Perhaps most surprisingly, substantial oxidation of propane (a three-carbon reactant) to maleic acid (a four-carbon product) is observed; maleic acid is the major product under some reaction conditions. The amount of maleic acid produced is strongly affected by both the exact catalyst composition and the reaction conditions. The presence of vanadium shifts the selectivity away from CO_x to maleic acid, and increasing the flow rate moves the selectivity toward the desired acrylic acid product. Formation of maleic acid from propane, although not previously reported in the literature, is

Table 7
Effects of different pretreatment conditions on reactivity

Catalyst (pretreatment)	Flow (mL min^{-1}) ^a	<i>T</i> (°C)	Conversion (%)		Selectivity (%)				STY ^b
			C ₄	O ₂	CO _x	Ac	AA	MA	
$\text{NbPMo}_{11}\text{V}$ (He)	4:2:4:5	380	0.4	8	42	19	4	25	6.3×10^{-4}
$\text{NbPMo}_{11}\text{V}$ (CO)	4:2:4:5	380	11.3	75	14	12	7	66	0.059
$\text{NbPMo}_{11}\text{V}$ (NH ₃)	4:2:4:5	380	1.4	36	86	2	0	0	0
$\text{NbPMo}_{11}\text{V}$ (H ₂)	4:2:4:5	380	3.4	44	70	9	3	15	7.8×10^{-3}
$\text{NbPMo}_{11}\text{Vpyr}$	32:16:32:40	380	14	95	9	5	3	80	0.76
$\text{NbPMo}_{11}\text{Vpyr}$ (CO)	27:16:32:40	380	12	84	51	5	3	40	0.27

^a *n*-Butane:oxygen:helium:water.

^b Space-time yield of maleic acid (mmol min^{-1} (g of catalyst)⁻¹).

Table 8
Catalyst reactivity using propane as a substrate

Catalyst	Conversion (%)		Selectivity (%) ^a					STY ^b
	C ₃	O ₂	CO _x	C ₃ ⁼	Ac	AA	MA	
PMo ₁₁ V ^c	0.4	3.4	30	54	4	0	0	0
NbPMo ₁₁ V ^c	1.4	5.7	22	44	16	10	0	1.39 × 10 ⁻³
PMo ₁₁ Vpyr ^c	3.4	10.1	10	37	30	17	0	5.55 × 10 ⁻³
NbPMo ₁₂ pyr ^c	25	100	79	1	2	2	14	0.008
NbPMo ₁₂ pyr ^d	18	95	65	1	3	6	21	0.067
NbPMo ₁₁ Vpyr ^d	21	76	11	0	23	49	15	0.623
PMo ₁₁ Nbpyr ^c	25	100	65	0	3	3	29	0.012
PMo ₁₁ Nbpyr ^d	8	55	45	0	8	17	23	0.16
(VO)PMo ₁₁ Nbpyr ^d	18	90	25	0	10	28	22	0.31

Some of the data in this table have been previously reported [15].

^a C₃, propane; CO_x, carbon oxides; C₃⁼, propene; Ac, acetic acid; AA, acrylic acid; MA, maleic acid.

^b Space-time yield of acrylic acid (mmol min⁻¹ (g of catalyst)⁻¹).

^c Flow rates: 8:4:8:10 mL min⁻¹ of propane:oxygen:helium:water at 380 °C.

^d Flow rates: 32:16:32:40 mL min⁻¹ of propane:oxygen:helium:water at 380 °C.

Table 9
Reactivity of NbPMo₁₁Vpyr under different conditions for propane

Flow (mL min ⁻¹) ^a	T (°C)	Conversion (%)		Selectivity (%)				Space-time yield ^b	
		C ₃	O ₂	CO _x	Ac	AA	MA	AA	MA
8:4:8:10	380	25	99	15	19	21	43	0.18	0.27
32:16:32:40	380	21	76	11	23	49	15	0.62	0.16
32:16:32:40	340	11	63	24	28	17	28	0.09	0.11
16:8:16:20	340	15	83	18	32	16	22	0.07	0.07

^a Propane:oxygen:helium:water.

^b Space-time yield of acrylic and maleic acid (mmol min⁻¹ (g of catalyst)⁻¹).

Table 10
Comparison of propane reactivity to literature data

Catalyst	Flow (mL min ⁻¹) ^a	T (°C)	Residence time (s)	Conv. C ₃ (%)	Sel. AA (%)	Yield AA	STY ^b AA	Ref.
MoSbVNbO _x	2:3.2:11.8:28	400	2.0	31	30	9	4.9 e-3	[9]
MoVNbTeO _x	0.6:2:7.4:8.8	380	1.9	80	61	49	0.018	[8]
CsFe(PMo ₁₁ VO ₄₀)	4.5:7.5:3:0	380	4.0	47	28	13	0.024	[34]
NbPMo ₁₁ Vpyr	3:8.6:18:21	380	0.24	10	29	3	0.009	This work
NbPMo ₁₁ Vpyr	32:16:32:40	380	0.1	21	50	11	0.62	This work

Some of the data in this table have been previously reported [15].

^a Propane:oxygen:helium:water.

^b Space-time yield of acrylic acid (mmol min⁻¹ (g of catalyst)⁻¹).

not unique to these catalysts. Reacting a similar propane-rich feed over a VPO catalyst also produces substantial amounts of maleic acid (data not shown). Additionally, oxidation of C₅ and higher hydrocarbons over VPO catalysts are known to produce maleic acid as a major product [24,25]. Plausible reaction mechanisms for the formation of maleic acid from propane have been previously presented [26]. In that study, experiments using ¹³C-labeled propane implicate a pathway of oxidative dehydrogenation of propane to propene followed by mostly acid-catalyzed dimerization to C₆ hydrocarbons. The C₆ hydrocarbons are then selectively oxidized to maleic acid.

The space-time yields for the NbPMo₁₂pyr and NbPMo₁₁Vpyr catalysts for maleic acid and acrylic acid compare well

with previously reported literature results. For butane, comparisons are included with VPO and other heteropolyacid-based-catalysts. NbPMo₁₂pyr has a productivity one order of magnitude greater than VPO as reported by Ledoux et al. [27]. Under oxygen-rich conditions the productivity of NbPMo₁₂pyr is within a factor of 4 of VPO, even though no attempt has been made to optimize the catalyst under these conditions. Most work on selective oxidation has been under oxygen-rich conditions; however, investigation of hydrocarbon-rich conditions has also been reported (see Hutchings [28] and references therein). In contrast to our catalyst system that is active under both hydrocarbon-rich and oxygen-rich conditions, Mota et al. have reported that VPO deactivates under hydrocarbon-rich conditions [29], al-

Table 11
 Reactivity of other substrates

Ethane									
Catalyst	Flow (mL min ⁻¹) ^a	T (°C)	Conversion		Selectivity ^b		Space-time yield ^c		Ref.
			C ₂	O ₂	C ₂ ⁼	Ac	C ₂ ⁼	Ac	
NbPMo ₁₁ Vpyr	4:2:4:5	380	5.7	9.6	59	13	3.0 × 10 ⁻²	6.5 × 10 ⁻³	This work
Mo _{0.73} V _{0.18} Nb _{0.09}	13.3:8.8:125.2:0	350	58	–	65	–	7.1 × 10 ⁻³	–	[5]
VO _x /TiO ₂	141.7:8.3:16.7:0	250	1	–	18	36	3.5 × 10 ⁻³	6.9 × 10 ⁻³	[6]
Mo _{0.73} V _{0.18} Nb _{0.09} ^d	6:3.6:14.4:0	350	32	–	44	2.5	3.9 × 10 ⁻¹	2.2 × 10 ⁻²	[37]
Mo ₁ V _{0.25} Nb _{0.12}	7.3:1.5:9.5:0.1	246	4.7	–	1	59	4.3 × 10 ⁻³	1.2 × 10 ⁻²	[38]
Pd _{0.0005} O _x ^e									
Isobutane									
Catalyst	Flow (mL min ⁻¹) ^f	T (°C)	Conversion		Selectivity ^g		Space-time yield ^c		Ref.
			Iso-C ₄	O ₂	MAA	MA	MAA	MA	
NbPMo ₁₁ Vpyr	28:14:28:35	380	13	98	1.7	3.9	1.3 × 10 ⁻²	2.9 × 10 ⁻²	This work
H ₃ PMo ₁₂ O ₄₀ pyr	1:4:15:10	300	22	–	52	–	1.6 × 10 ⁻³	–	[14]
Toluene									
Catalyst	Flow (mL min ⁻¹) ^h	T (°C)	Conversion		Selectivity ⁱ		Space-time yield ^c		Ref.
			C ₇	O ₂	BzA	BA	BzA	BA	
NbPMo ₁₂ pyr	0.16:2:4:5	380	26	55	8	29	5.6 × 10 ⁻⁴	2.2 × 10 ⁻³	This work
Ag _{1.2} V ₃ Ce _{0.15} O _{8+x}	3:45.7:179.7:0	370	5	–	30	40	4.5 × 10 ⁻³	6 × 10 ⁻³	[39]

^a Ethane:oxygen:inert:water.

^b C₂, ethane; C₂⁼, ethene; Ac, acetic acid.

^c Space-time yield (mmol min⁻¹ (g of catalyst)⁻¹).

^d P_{tot} = 2.0 MPa.

^e P_{tot} = 1.5 MPa.

^f Isobutane:oxygen:helium:water.

^g Iso-C₄, isobutane; MAA, methacrylic acid; MA, maleic acid.

^h Toluene:oxygen:helium:water.

ⁱ C₇, toluene; BzA, benzoic acid; BA, benzaldehyde.

though by doping the VPO catalyst with cobalt some activity could be restored [30]. Addition of niobium to VPO under conventional oxygen-rich conditions has also been investigated. The niobium allows more rapid activation of the catalysts as well as enhancing *n*-butane conversion while not affecting the selectivity to maleic anhydride [31,32]. It is also interesting to note that the NbPMo₁₂pyr catalyst, containing no vanadium, is extremely active for butane to maleic acid; previous effective catalysts for this reaction have almost exclusively contained vanadium [1].

Heteropolyacid catalysts have also been examined for the production of maleic acid from butane. To induce activity for the reaction, two approaches have been used: (1) incorporation of vanadium into the structure [10], and (2) preparation of vanadyl-exchanged species in combination with other cations [4,11,33]. In both cases, the presence of vanadium has been crucial to obtaining useful activity. The niobium/pyridine polyoxometalate catalysts have activity two orders of magnitude better than either the structural or exchanged vanadium containing heteropolyacid-based catalysts reported in the literature. In addition, vanadium is not required for this high activity, and when present does not cause a dramatic difference in the activity.

Similar literature comparisons for propane reactivity over both heteropolyacid-based catalysts and MoVNb mixed-metal oxides are given in Table 10. The MoVNb mixed-metal oxide systems of Ushikubo et al. and Takahashi et al. have received significant attention of late as a large step forward in the production of acrylic acid from propane [8,9]. The literature data reported in Table 10 are all under different conditions, and it is therefore difficult to make precise comparisons. However, it is clear that the NbPMo₁₁Vpyr catalysts reported here have exceptional productivity for the conversion of propane to acrylic acid. The selectivity to acrylic acid for NbPMo₁₁Vpyr is less than MoVNbTeO_x, but this is partly due to the coproduction of maleic acid. Similar to the butane results, these catalysts are not as effective under oxygen-rich conditions, although the productivity is still within a factor of 2 of the Mitsubishi MoVNbTeO_x catalyst. When compared to the heteropolyacid-based systems in the literature [13,34], the NbPMo₁₁Vpyr system is much more productive for acrylic acid formation.

In contrast to results for butane to maleic acid reported here, effective formation of acrylic acid from propane appears to require the presence of vanadium in the catalyst. The vanadium-free catalyst, while also extremely active, has selectivity to CO_x of almost 80%. Similar results were

observed for the samples with niobium synthesized in the Keggin unit and no ion-exchanged vanadium. These trends are not unprecedented, as a synergistic effect of niobium and vanadium for the formation of acrylic acid over MoVNbTe mixed-metal oxides has been previously reported [35,36]. These authors conclude that higher activity can be correlated with catalysts containing Nb⁵⁺ ions, but only if vanadium is also present in the sample. With mixed-metal oxides, it was suggested that the role of the niobium ions could be related to the formation of an active phase with low crystallinity and higher surface area. For the samples used in the present study, addition of niobium to a PMo₁₁Vpyr material actually reduced the surface area of the catalyst. From the activity results, it is observed that NbPMo₁₂pyr has good activity, but very low selectivity to the acids. By comparison, NbPMo₁₁Vpyr has similar activity but greatly increased selectivity. Also, PMo₁₁Nbpyr exhibits good activity and poor selectivity while (VO)PMo₁₁Nbpyr has both good activity and selectivity. Since the PMo₁₁Vpyr sample does not have nearly the activity of NbPMo₁₁Vpyr, the presence of niobium is responsible for increased propane activation. However, only when vanadium is incorporated into the sample does the acid selectivity improve. Therefore, both components are critical to a highly active and selective catalyst. It is unclear whether the niobium and vanadium act directly as part of the atomic arrangement of the active site or if they act indirectly by stabilizing the formation of an active phase. Ai has observed similar effects for *n*-butane oxidation of heteropolyacid-based catalysts where multiple species were required to obtain active and selective catalysts [11].

In addition to butane and propane, the NbPMo₁₁V materials are capable of catalyzing the selective oxidation of other substrates. Examples include ethane, isobutane, and toluene. For ethane, the main products are ethylene and acetic acid. The observed space-time yield of ethylene for NbPMo₁₁Vpyr is greater by four times that reported by Thorsteinson et al. for a MoVNb mixed-metal oxide [5]. Formation of acetic acid is comparable to that of ethylene. Similar space-time yields of acetic acid at lower temperatures have been reported in the literature, but this may result from these samples being on high surface area supports [6]. Other data for the MoVNb-based systems at elevated pressures and specifically designed to produce either ethylene or acetic acid are also shown [37,38]. Comparisons to these results are even more difficult due to the higher pressures involved (2.0 and 1.5 MPa, respectively). In contrast to the propane reaction, no evidence for carbon–carbon coupling to C₃ or higher products is observed.

For isobutane, the activity is very similar to that of butane. However, the selectivity to CO_x is 86% while selectivity to the desired product of methacrylic acid is only around 2%. The productivity of methacrylic acid is an order of magnitude greater than reported by Li and Ueda; however, they operated at a temperature of 300 °C [14]. A reduction in reaction temperature may minimize the side reactions of isobutane to CO_x and shift selectivity to the desired prod-

uct for our system. Toluene was also investigated to examine selective side-chain oxidation of an aromatic species. The major product is CO_x with selectivity to benzoic acid and benzaldehyde being 8 and 29%, respectively. Space-time yields are lower than those reported by Yan and Anderson for AgVCe mixed-metal oxides [39]. Attempts to activate methane (380 °C ≤ *T* ≤ 460 °C) produce only small amounts of complete oxidation products.

The most active catalysts, NbPMo₁₂pyr and NbPMo₁₁Vpyr, involve three main components: (1) a central oxomolybdate cluster, (2) an exchange metal cation, and (3) an organic base. The role of each in gaining reactivity can be separately investigated. Catalysts based on metal oxides of several different types were studied: first, the bulk metal oxide and a physical mixture of MoO₃, V₂O₅, Nb₂O₅, and pyridine; second, the discrete metal oxide cluster octamolybdate; third, several different polyoxometalate structures, including the Keggin, Wells–Dawson, and Strandberg units that all contain the MoO_x clusters and a heteroatom in different geometries. The effect of changing the heteroatom while leaving the structure the same was also examined by comparing a silicomolybdate to the corresponding phosphomolybdate.

Molybdenum trioxide and the physical mixture of metal oxides both exhibit poor activity for butane oxidation in comparison to NbPMo₁₂pyr; this strongly suggests the active phase is more complex than the combination of bulk oxide structures. The structures of MoO₃ and Mo₈O₂₆⁴⁻ (octamolybdate) differ in their arrangement of molybdenum oxide octahedra; MoO₆ are corner-bound through an infinite network in MoO₃ and exist in discrete clusters in Mo₈O₂₆⁴⁻. In the presence of niobium and pyridine the octamolybdate exhibits good selectivity; however, the presence of a central phosphorus heteroatom in the Keggin unit of NbPMo₁₂pyr enhances catalyst performance substantially. The enhancement in reactivity may be due to the ability of the phosphorus atom to stabilize the structure by inhibiting the phase transition of the material into catalytically inert MoO₃. By TGA-DSC analysis (not shown), NbMo₈pyr decomposes to MoO₃ at 290 °C, while PMo₁₂ decomposes to MoO₃ at 440 °C. Interestingly, NbPMo₁₂pyr does not decompose to MoO₃ at all. Clearly, the presence of the phosphorus heteroatom helps stabilization of the active structure in the range of reaction temperatures. A more detailed discussion of the decomposition characteristics of the catalysts is presented in Part II [23].

Comparison of reactivity results for NbPMo₁₂pyr and PMo₁₁Nbpyr indicates that the location of niobium in as-synthesized samples, either ion-exchanged or incorporated in the structure, has no significant effect on productivity. These data suggest that niobium is mobile during the pretreatment; EXAFS results supporting this conclusion are presented in the following paper [23].

The nature of the heteroatom (phosphorus or silicon) in the heteropolyanion has a significant effect on catalyst performance. The stabilizing effect of phosphorus on the struc-

ture during catalyst pretreatment is responsible in part for the formation of the active phase. By TGA-DSC analysis (data not shown), silicomolybdic acid and phosphomolybdic acid differ in their thermal stabilities. Significant decomposition takes place for the SiMo_{12} -based catalyst at pretreatment temperatures and results in a mixture of metal oxides (this is not the case for PMo_{12} -based catalysts). The activity and selectivity exhibited by $\text{NbSiMo}_{12}\text{pyr}$ and by the physical mixture of mixed oxides for *n*-butane oxidation are comparable (Table 5), supporting this argument.

The second component of the active catalyst is the exchanged-metal cation. Elements near niobium in the periodic table as well as other elements used in mixed-metal oxides for propane oxidation such as antimony and bismuth were investigated. Molybdenum and titanium show activity of about one-half that of niobium. In contrast, vanadium is almost an order of magnitude less active. In fact, the sample with only pyridine and no exchange cation is more active than the vanadium-exchanged sample. The results of our vanadium-exchanged catalyst and the $\text{PMo}_{11}\text{Vpyr}$ catalyst show similar space-time yields of maleic acid. This demonstrates that the location of vanadium in the as-synthesized materials has little effect on reactivity and suggests that vanadium is mobile during activation and reaction; indeed, regardless of its initial location, once activated, the vanadium likely plays the same role in both catalysts. The initial oxidation state of the exchange cation does not appear important since the three most active catalysts have 5+, 4+, and 6+ oxidation states (Nb, Ti, and Mo, respectively). It is also interesting that zirconium gives better activity than vanadium since zirconium is considered much less susceptible to oxidation-reduction cycling than vanadium [40].

An additional aspect of the exchange-metal cation involves the amount of niobium present. Reactivity results suggest that a ratio of about 0.30 niobium atoms per Keggin unit is optimal. Since more pyridine is exchangeable with catalysts that contain less niobium, and since pyridine also is critical for enhancing activity, the ratio of 0.30 probably represents a balance between the two effects.

The third component of the active catalyst is the organic base. As further discussed in Part II [23], the role of the base is to act as an in situ reductant to reduce both molybdenum and niobium. An attempt was made to perform the same role by using the gas phase reducing agents CO, NH_3 , and H_2 . Although CO did increase the activity of pyridine-free $\text{NbPMo}_{11}\text{V}$, it is still one order of magnitude less active than the sample synthesized with pyridine. The samples pretreated in H_2 and NH_3 are even less active. Additionally, pretreating a pyridine-containing catalyst in CO did not further increase the activity. Under CO, TGA-DSC data indicate that the pyridine-free sample first decomposes to MoO_3 at 440 °C (which is above our pretreatment temperature), and then subsequently undergoes reduction. In contrast, the pyridine-containing sample reduces at lower temperatures without first going through MoO_3 . Therefore,

even though activity can be improved using a gaseous reductant, it still cannot completely replicate the role of the pyridine.

In addition to pyridine, other organic bases have been investigated. Although other bases are capable of activating the catalyst, none performed better than pyridine. Attempts to correlate activity with characteristics of the base such as molecular size and $\text{p}K_a$ were unsuccessful.

5. Conclusions

A substrate versatile catalyst for the selective oxidation of light alkanes has been developed. The catalysts are niobium and pyridine-exchanged salts of molybdophosphoric acid and molybdovanadophosphoric acid ($\text{NbPMo}_{12}\text{pyr}$ and $\text{NbPMo}_{11}\text{Vpyr}$). These catalysts are active and selective for the selective oxidation of propane and *n*-butane over a wide temperature range and under both hydrocarbon-rich and oxygen-rich reaction conditions. The catalysts that contain both niobium and pyridine are very active and selective. For the selective oxidation of *n*-butane to maleic acid, the presence of vanadium does not appear to significantly influence the reactivity. In contrast, for the selective oxidation of propane to acrylic acid, the presence of vanadium significantly affects the selectivity to the desired product. Surprisingly, the selective oxidation of propane also leads to the production of maleic acid as a major product under certain reaction conditions.

Although metal cations other than niobium show some activity for selective oxidation, none appear better than niobium. The central phosphorus atom of the polyoxometalate is important. If the phosphorus is not present or replaced by another heteroatom, productivities are much lower. For both propane and *n*-butane, the synthesized location of the niobium (structural or ion-exchanged) does not have a large effect on reactivity. Similarly for propane, the synthesized location of vanadium has minimal effect on activity.

For the selective oxidation of *n*-butane, the productivity of the catalyst reported here is greater than that of VPO. With propane, the productivity of acrylic acid exceeds that of MoVNbTeO_x . The catalysts are also active for selective oxidation of other substrates such as ethane, isobutane, and toluene.

Acknowledgments

This work was funded by BP. We thank Larry Henling and Michael Day (Beckman Institute, California Institute of Technology) for single-crystal X-ray diffraction.

References

- [1] G. Centi, F. Cavani, F. Trifiro, *Selective Oxidation by Heterogeneous Catalysis*, Kluwer Academic/Plenum, New York, 2001.

- [2] F. Cavani, F. Trifiro, *Catalysis* (1994) 247.
- [3] B.K. Hodnett, *Heterogeneous Catalytic Oxidation*, Wiley, Chichester, 2000.
- [4] M. Ai, *J. Mol. Catal. A: Chem.* 114 (1996) 3.
- [5] E.M. Thorsteinson, T.P. Wilson, F.G. Young, P.H. Kasai, *J. Catal.* 52 (1978) 116.
- [6] L. Tessier, E. Bordes, M. Gubelmann-Bonneau, *Catal. Today* 24 (1995) 335.
- [7] M.M. Lin, *Appl. Catal. A* 207 (2001) 1.
- [8] T. Ushikubo, H. Nakamura, Y. Koyasu, S. Wajiki, US Patent 5,380,933 Mitsubishi Kasei, 1995.
- [9] M. Takahashi, X. Tu, T. Hirose, M. Ishii, US Patent 6,060,422 Toagosei Co. Ltd., 2000.
- [10] G. Centi, V. Lena, F. Trifiro, D. Ghoussoub, C.F. Aissi, M. Guelton, J.P. Bonnelle, *J. Chem. Soc. Faraday Trans.* 1990 (1990) 2775.
- [11] M. Ai, in: 8th International Congress on Catalysis, Vol. 5, Dechema, Berlin, 1994, p. 475.
- [12] B.B. Bardin, R.J. Davis, *Appl. Catal. A* 185 (1999) 283.
- [13] W. Ueda, Y. Suzuki, *Chem. Lett.* (1995) 541.
- [14] W. Li, W. Ueda, in: R.K. Grasselli, S.T. Oyama, A.M. Gaffney, J.E. Lyons (Eds.), *3rd World Congress on Oxidation Catalysis*, Elsevier, Amsterdam, 1997, p. 433.
- [15] M.E. Davis, C.J. Dillon, J.H. Holles, J. Labinger, *Angew. Chem. Int. Ed.* 41 (2002) 858.
- [16] G.A. Tsigdinos, C.J. Hallada, *Inorg. Chem.* 7 (1968) 437.
- [17] R. Massart, R. Contant, J.-M. Fruchart, J.-P. Ciabrini, M. Fournier, *Inorg. Chem.* 16 (1977) 2916.
- [18] R. Strandberg, *Acta Chem. Scand.* 27 (1973) 1004.
- [19] L. Pettersson, I. Andersson, L.-O. Ohman, *Acta Chem. Scand.* A 39 (1985) 53.
- [20] P. Gili, P. Martin-Zarza, G. Martin-Reyes, J.M. Arrieta, G. Madariaga, *Polyhedron* 11 (1992) 115.
- [21] E.M. McCarron III, J.F. Whitney, D.B. Chase, *Inorg. Chem.* 23 (1984) 3275.
- [22] J.S. Min, M. Misono, A. Taguchi, N. Mizuno, *Chem. Lett.* (2001) 28.
- [23] C.J. Dillon, J.H. Holles, R.J. Davis, J.A. Labinger, M.E. Davis, *J. Catal.*, in press.
- [24] F. Cavani, F. Trifiro, *Appl. Catal. A* 157 (1997) 195.
- [25] F. Cavani, A. Colombo, F. Trifiro, G.J. Hutchings, *Catal. Lett.* 43 (1997) 241.
- [26] C.J. Dillon, J.H. Holles, M.E. Davis, J.A. Labinger, *Catal. Today*, in press.
- [27] M.J. Ledoux, C. Crouzet, C. Pham-Huu, V. Turines, K. Kourtakis, P.L. Mills, J.J. Lerou, *J. Catal.* 203 (2001) 495.
- [28] G.J. Hutchings, *Appl. Catal.* 72 (1991) 1.
- [29] S. Mota, M. Abon, J.C. Volta, J.A. Dalmon, *J. Catal.* 193 (2000) 308.
- [30] S. Mota, J.C. Volta, G. Vorbeck, J.A. Dalmon, *J. Catal.* 193 (2000) 319.
- [31] P.G. Pries de Oliveira, J.G. Eon, M. Chavant, A.S. Riché, V. Metin, S. Caldarelli, J.C. Volta, *Catal. Today* 57 (2000) 177.
- [32] A.M. Duarte de Farias, W.A. de Gonzalez, P.G. Pries de Oliveira, J.-G. Eon, J.-M. Herrmann, M. Aouine, S. Loricant, J.C. Volta, *J. Catal.* 208 (2002) 238.
- [33] M. Ai, *J. Catal.* 85 (1984) 324.
- [34] N. Mizuno, D. Suh, W. Han, T. Kudo, *J. Mol. Catal. A: Chem.* 114 (1996) 309.
- [35] P. Botella, B. Solsona, A. Martinez-Arias, J.M. Lopez Nito, *Catal. Lett.* 74 (2001) 149.
- [36] P. Botella, J.M. Lopez Nito, B. Solsona, *Catal. Lett.* 78 (2002) 383.
- [37] K. Ruth, R. Burch, R. Kieffer, *J. Catal.* 175 (1998) 27.
- [38] D. Linke, D. Wolf, M. Baerns, O. Timpe, R. Schlögl, S. Zeyß, U. Dingerdissen, *J. Catal.* 205 (2002) 16.
- [39] Z.-G. Yan, S.L.T. Andersson, *J. Catal.* 131 (1991) 350.
- [40] C.S.G. Phillips, R.J.P. Williams, *Inorganic Chemistry*, Oxford Univ. Press, Oxford, 1966.